

A Photon Cloud Induced from an Axion Cloud

Zi-Yu Tang^{1,*} and Eleftherios Papantonopoulos^{2,†}

¹*Cosmology, Gravity and Astroparticle Physics Group,
Center for Theoretical Physics of the Universe,
Institute for Basic Science, Daejeon 34126, Korea*

²*Physics Division, School of Applied Mathematical and Physical Sciences,
National Technical University of Athens, 15780 Zografou Campus, Athens, Greece.*

It is known that the axion-photon coupling can lead to quantum stimulated emission of photons and classic exponential amplification of electromagnetic (EM) fields at half the axion mass frequency, when the axion density or the coupling constant is sufficiently large. In this work, we studied the EM photon cloud induced from an axion cloud around a Kerr black hole in the first order of the coupling constant classically. In the presence of a static EM background (like Wald extended solution) valid in realistic astrophysical environment, we found that an EM photon cloud emerges, oscillating at the same frequency as the axion cloud and growing exponentially in accordance with the axion cloud when the superradiant condition for the axion field is satisfied. Notably, the first-order study indicates that this photon cloud exists with no threshold for the coupling constant. The evolution of the EM photon cloud with time and azimuthal angle is obtained analytically while the cross-sectional distribution is solved numerically. Intriguingly, the induced EM field exhibits significantly different symmetries in contrast to the background EM field, which may serve as an indication of the existence of both an axion cloud and axion-photon coupling. Furthermore, in the near horizon region, the induced EM field has some overlap with the photon region as expected.

I. INTRODUCTION

Axions or axion-like particles were introduced to solve the strong CP problem arising in QCD as it was found a discrepancy between the observed and predicted magnitude of the neutron electric dipole moment in the strong sector of the standard model [1–3]. Also axions appear in supersymmetric theories, and theories with extra dimensions including string theory from the compactification of the extra dimensions [4–6]. In (3+1)-dimensional case, a type called string-model independent axion [7, 8] is dual to the field strength of the Kalb-Ramond, spin-one, antisymmetric tensor field, and plays the role of a totally antisymmetric torsion in the geometry.

Recently there are extensive experimental and observational efforts to find axionic imprints. Superradiant mechanisms can give us information about their existence as axions form dense clouds around spinning black holes [9]. The superradiance mechanism is a very well known method of extracting energy from a rotating black hole [10–12]. It was shown by Penrose [13] that if a particle accretes into a Kerr black hole then energy can be extracted from the black hole. It was shown by Misner [14] that there is a constrain of the frequency of scatter waves off the black hole to be less than the rotational frequency of the black hole. Then if this constrained condition is satisfied it was shown by Teukolsky [15] that this energy extraction mechanism also works in the case of EM and gravitational waves, though the Kerr solution remains stable under massless scalar, EM and gravitational perturbations without reflection.

It is well known that an isolated black hole cannot have an EM field unless it is endowed with a net electric charge. Therefore, for an isolated black hole to have some EM effects there should be a mechanism for charging it. If a black hole is in an astrophysical environment with a galactic magnetic field, EMs produced by external sources may charge it. In [16] an axisymmetric black hole which was placed in an originally uniform magnetic field and no significant field enhancement effects were found. However, if the black hole is rotating, the rotational effects of the black hole, produce electric fields near the black hole. Extraction of energy and charge from a black hole was studied in [17]. The superradiance effects and the multimessenger signals of an EM field were studied in [18, 19].

* tangziyu@ibs.re.kr

† lpapa@central.ntua.gr

It was shown in [20] that the presence of light scalars like axions can trigger superradiant instabilities around Kerr BHs and lead to the deposition of the black hole rotation energy in a cloud. Also it was shown in [21] that the presence of an axion field can lead to the reversal of rotation in Kerr black holes. It was also shown that instabilities are generated and a fraction of the cloud energy is transferred to EM blasts. The resulting large energy density of the cloud rotates around the black hole, and results to a monochromatic gravitational wave radiation that drain the cloud over parametrically longer times [22].

Although the axion-photon coupling is expected to be very weak, it was suggested that the quantum stimulated emission of photons can be generated at large enough axion number [23, 24], and conjectured that blasts of light could be emitted from black hole systems [25, 26]. Recently at classical level, it was shown that EM fields can be exponentially amplified in Kerr-axion cloud system, when the amplitude of the axion cloud multiplied by the coupling constant is larger than a critical value [20]. Even in the presence of plasma, the EM instability is still controlled by the axionic coupling [9]. In [27], the origin of the instability from the axion-photon coupling was analyzed in flat space through the Mathieu equation, and it was found that a background EM field can produce an axion profile around a Kerr black hole perturbatively. On the other side, from the European Horizon Telescope (EHT) observation of the polarimetric measurements of M87*, stringent constraints on the axion-photon coupling constant were given in the mass range of $\sim (10^{-21} - 10^{-20})\text{eV}$ from the azimuthal distribution of electric vector position angle [28]. Furthermore, the deviation of photon geodesics due to oscillating metric perturbations induced from the superradiant clouds was predicted in [11].

In this work we studied the EM photon cloud induced from an axion cloud via the axion-photon coupling surrounding a Kerr black hole. In the first order of the coupling constant, we found that a background EM field is necessary to have a first-order induced EM structure, and if it is stationary then the frequency of the induced photon cloud will be the same as the frequency of the axion cloud. It means that it grows or decays in accordance with the axion cloud when the superradiant condition for the axion field is satisfied or not, while the oscillating frequency is also the same. It is well known that the timescale of the superradiant instability is much larger than the timescale of the oscillation, therefore we can ignore the growth of the amplitude and focus on the oscillating part. It is surprising that even with very small couplings, no threshold is needed, there exists an oscillating photon cloud at the same frequency as the axion cloud and it will grow exponentially when the axion cloud is growing. Whereas in the previous studies, without a background EM field, a threshold for the amplitude of the axion cloud multiplied by the coupling constant and an initial EM pulse are both required, otherwise there is no instability and the initial EM fluctuation will decay exponentially. In contrast, for the dark photon-photon coupling case, a dark photon cloud can transfer its energy to form a rotating EM field directly [18].

The work is organized as follows. Firstly in Sec. II we study the basic field equations in the first-order of the coupling constant, then in Sec. III we show how an EM photon cloud is induced from the axion cloud in the presence of an EM background and discuss symmetries. Moreover, in Sec. IV we study the induced electric and magnetic fields respectively, and in Sec. V we analyze the symmetries of most quantities and confirm the parity violation. Finally in Sec. VI we conclude.

II. FIRST-ORDER ANALYSIS OF THE AXION-PHOTON COUPLING

In this work, we consider the interaction between an axion cloud and the EM field around a Kerr black hole with the action

$$S = \int d^4x \sqrt{-g} \left[\frac{R}{2\kappa} + \mathcal{L}_m \right], \quad (1)$$

$$\mathcal{L}_m = -\frac{1}{4}F_{\mu\nu}F^{\mu\nu} - \frac{1}{2}\nabla_\mu\phi\nabla^\mu\phi - \frac{1}{2}\mu_1^2\phi^2 - \frac{k_a}{2}\phi F_{\mu\nu}^*F^{\mu\nu}, \quad (2)$$

where the axion field ϕ is a real pseudo scalar field with mass $m_a \equiv \mu_1\hbar$, k_a is the coupling constant, $F_{\mu\nu} \equiv \nabla_\mu A_\nu - \nabla_\nu A_\mu$ is the electromagnetic field strength tensor and $*F^{\mu\nu} \equiv \frac{1}{2}\epsilon^{\mu\nu\rho\sigma}F_{\rho\sigma}$ is the dual field strength tensor. The $\epsilon^{\mu\nu\rho\sigma} \equiv \frac{1}{\sqrt{-g}}E^{\mu\nu\rho\sigma}$ and $E^{\mu\nu\rho\sigma}$ is the totally antisymmetric Levi-Civita symbol with $E^{0123} = 1$. We use geometrized units $c = G = 1$ unless otherwise specified.

By variation of the above action, we obtain the basic field equations

$$\nabla^\mu \nabla_\mu \phi - \mu_1^2 \phi - \frac{k_a}{2} F_{\mu\nu}^* F^{\mu\nu} = 0 , \quad (3)$$

$$\nabla_\nu F^{\mu\nu} + 2k_a \nabla_\nu \phi^* F^{\mu\nu} = 0 , \quad (4)$$

$$R_{\mu\nu} - \frac{1}{2} g_{\mu\nu} R = \kappa \left(g_{\mu\nu} \mathcal{L}_m - 2 \frac{\delta \mathcal{L}_m}{\delta g^{\mu\nu}} \right) \equiv \kappa T_{\mu\nu} , \quad (5)$$

with

$$\frac{\delta \mathcal{L}_m}{\delta g^{\mu\nu}} = -\frac{1}{2} F^\sigma{}_\mu F_{\sigma\nu} - \frac{1}{2} \nabla_\mu \phi \nabla_\nu \phi - 2k_a \phi F^\sigma{}_\nu{}^* F_{\sigma\mu} . \quad (6)$$

In our study, the Kerr geometry is fixed as the background, since the backreactions of both axion cloud and the EMs on the metric are in the second-order of the fluctuations. We expand the scalar and EM field equations to the first-order of the coupling constant k_a

$$\nabla^\mu \nabla_\mu \phi_{(0)} - \mu_1^2 \phi_{(0)} + k_a \left(\nabla^\mu \nabla_\mu \phi_{(1)} - \mu_1^2 \phi_{(1)} - \frac{1}{2} F_{\mu\nu}^{(0)*} F^{\mu\nu}_{(0)} \right) + \mathcal{O}(k_a^2) = 0 , \quad (7)$$

$$\nabla_\nu F^{\mu\nu}_{(0)} + k_a \left(\nabla_\nu F^{\mu\nu}_{(1)} + 2 \nabla_\nu \phi_{(0)}^* F^{\mu\nu}_{(0)} \right) + \mathcal{O}(k_a^2) = 0 , \quad (8)$$

which clearly shows that at zero-order the axion cloud and the EM field obey their own field equations respectively, and at first-order the existence of a background EM field can give a substructure on the axion cloud while the existence of both axion cloud and a background EM field can induce an extra EM field in order of k_a . The first-order backreaction on the axion cloud has been studied in [27]. In this work, we focus on the EM field induced from the axion cloud in the presence of a background EM field.

The Kerr metric in Boyer-Lindquist (BL) coordinates is

$$ds^2 = -\frac{1}{\Sigma} (\Delta_r - a^2 \sin^2 \theta) dt^2 + \frac{\Sigma}{\Delta_r} dr^2 + \Sigma d\theta^2 + \frac{\Gamma}{\Sigma} \sin^2 \theta d\varphi^2 - \frac{4aMr}{\Sigma} \sin^2 \theta dt d\varphi , \quad (9)$$

where

$$\Sigma = r^2 + a^2 \cos^2 \theta , \quad (10)$$

$$\Delta_r = r^2 - 2Mr + a^2 , \quad (11)$$

$$\Gamma = (a^2 + r^2)^2 - \Delta_r a^2 \sin^2 \theta . \quad (12)$$

For the background EM field we consider the extended Wald solution

$$A_\mu^{(0)} = A_\mu^{\text{Wald}} = \frac{B_0 \sin^2 \theta}{2\Sigma} (-2aMr, 0, 0, \Gamma) , \quad A_{(0)}^\mu = A_{\text{Wald}}^\mu = \left(0, 0, 0, \frac{B_0}{2} \right) , \quad (13)$$

which describes the equilibrium state of the black hole absorbing charges and discharging processes from the surroundings of astrophysical environments such as the accretion disk, plasma and the interstellar medium [16]. It is worth noting that this extended Wald solution is still an exact solution in Kerr geometry.

For the axion cloud part, the bound states in Kerr metric can be obtained analytically in approximation when the fine structure constant $\alpha_1 \equiv GM\mu_1/c = M\mu_1 \ll 1$ in separable form as

$$\phi_{(0)} = e^{-i\omega t + im\varphi} S_{lm}(\theta) R_{lm}(r) \quad (14)$$

with $\omega = \omega_R + i\omega_I$ that [29]

$$\omega_R \simeq \mu_1 \left(1 - \frac{\alpha_1^2}{2(n+l+1)^2} \right) , \quad (15)$$

$$\omega_I \simeq \frac{1}{\gamma_{nlm} M} \left(\frac{am}{M} - 2\mu_1 r_+ \right) \alpha_1^{4l+5} \quad (16)$$

where γ_{nlm} is a constant, n is the principal quantum number, and l corresponds to the orbital angular momentum quantum number. The condition for the superradiance to occur $\mu_1 < \frac{am}{2Mr_+} = m\Omega_H$ is equivalent to $\alpha_1 < \frac{am}{2r_+} = \frac{ma}{2M(1+\sqrt{1-a^2/M^2})}$.

As we can see in eq. (8), since the background EM field $F_{\mu\nu}^{(0)}$ is independent of time t and azimuthal angle φ , therefore the induced first-order EM field in form $F_{(1)}^{\mu\nu} \sim e^{-i\omega_1 t + im_1 \varphi}$ must have same frequency as the axion field (14) that $\omega_1 = \omega$ and $m_1 = m$. It means that the induced EM field grows or decays in accordance with the axion cloud when the superradiant condition for the axion field is satisfied or not, while the oscillating frequency is also the same. It is well known that the timescale of the superradiant instability is much larger than the timescale of the oscillation, therefore we can ignore the growth of the amplitude and focus on the oscillating part.

It is necessary to clarify the difference of the EM frequencies. Turning back to the original Klein-Gordon equation (3), an axion field evolving as $\phi \sim e^{-i\omega t + im\varphi}$ would lead to EM field as $F_{\mu\nu} \sim e^{-i\omega_{EM} t + im_{EM} \varphi}$ at half frequency of the axion field $\omega_{EM} = \omega/2$. While if we look at the EM field equation (4), we cannot get a direct relation between the axion frequency and the EM frequency.

In quantum stimulated case [23], the half frequency was explained as the axion decay channel is into two photons resulting the photon energy at $E = m_a/2$. Also, the numerical evolution results [9, 20] gave EM oscillation frequency at half the axion mass frequency for supercritical couplings. In [27], the origin of the instability was analyzed in flat space through the Mathieu equation, which predicts instabilities for $\omega_{EM} = \mu_1/2, \mu_1, 3\mu_1/2, \dots$. However in [9] the frequency peaks at $\mu_1, 2\mu_1, \dots$ were absent, and for high axionic couplings in dense plasmas $\omega_p > \mu_1/2$ the frequency centers at $\omega_{EM} = \mu_1$ instead of the usual $\omega_{EM} = \mu_1/2$, suggesting that the axion decay mechanism into two photons is forbidden and changes to process $\phi + \phi \rightarrow \gamma + \gamma$. Our understanding is that the half frequency appearing in classically numerical studies is because the main energy transfer from the axion cloud to EM field happens through the Klein-Gordon equation (3), so that even in curve spacetime we can still have a simple relation observed directly from the equation as we have analyzed previously.

III. A PHOTON CLOUD INDUCED FROM AN AXION CLOUD

Next, we try to solve the first-order induced EM field $F_{(1)}^{\mu\nu}$ in the Newman-Penrose (NP) formalism, in which using the Kinnersley's null tetrad [30]

$$l^\mu = \left(\frac{r^2 + a^2}{\Delta_r}, 1, 0, \frac{a}{\Delta_r} \right), \quad n^\mu = \frac{1}{2\Sigma} (r^2 + a^2, -\Delta_r, 0, a), \quad m^\mu = \frac{1}{\sqrt{2}(r + ia \cos \theta)} \left(ia \sin \theta, 0, 1, \frac{i}{\sin \theta} \right), \quad (17)$$

we can construct three NP components

$$\varphi_0 = F_{\mu\nu} l^\mu m^\nu, \quad \varphi_1 = \frac{1}{2} F_{\mu\nu} (l^\mu n^\nu + \bar{m}^\mu m^\nu), \quad \varphi_2 = F_{\mu\nu} \bar{m}^\mu n^\nu, \quad (18)$$

where φ_0 is the ingoing radiation with spin weight $s = 1$ and φ_2 represents outgoing radiation with spin weight $s = -1$. Note that there are only two real degree of freedoms though the three components are complex. The EM tensor can be reconstructed as

$$F_{\mu\nu} = 2\varphi_0 \bar{m}_{[\mu} n_{\nu]} + 2\bar{\varphi}_0 m_{[\mu} n_{\nu]} + 2(\varphi_1 + \bar{\varphi}_1) n_{[\mu} l_{\nu]} + 2(\varphi_1 - \bar{\varphi}_1) m_{[\mu} \bar{m}_{\nu]} + 2\varphi_2 l_{[\mu} m_{\nu]} + 2\bar{\varphi}_2 l_{[\mu} \bar{m}_{\nu]}. \quad (19)$$

We derived the perturbation equation for electromagnetic field with sources in NP formalism [15]

$$(D - 2\rho) \varphi_1 - (\bar{\delta} + \pi - 2\alpha) \varphi_0 + \kappa \varphi_2 = -\frac{1}{2} J_k, \quad (20)$$

$$(\delta - 2\tau) \varphi_1 - (\Delta + \mu - 2\gamma) \varphi_0 + \sigma \varphi_2 = -\frac{1}{2} J_m, \quad (21)$$

$$(D - \rho + 2\varepsilon) \varphi_2 - (\bar{\delta} + 2\pi) \varphi_1 + \lambda \varphi_0 = -\frac{1}{2} J_{\bar{m}}, \quad (22)$$

$$(\delta - \tau + 2\beta) \varphi_2 - (\Delta + 2\mu) \varphi_1 + \nu \varphi_0 = -\frac{1}{2} J_{\bar{m}}, \quad (23)$$

and obtained the decoupled equation for the NP scalar φ_1

$$[\Delta D + (\bar{\mu} - \mu - \gamma - \bar{\gamma}) D - \bar{\delta}\delta + (\bar{\tau} + 2\alpha)\delta] \frac{\varphi_1}{\rho^2} = [\Delta + (\bar{\mu} - \mu - \gamma - \bar{\gamma})] \frac{-J_l}{2\rho^2} + [\bar{\delta} - (\bar{\tau} + 2\alpha)] \frac{-J_m}{2\rho^2}, \quad (24)$$

where $D \equiv l^a \nabla_a$, $\Delta \equiv n^a \nabla_a$, $\delta \equiv m^a \nabla_a$, $\bar{\delta} \equiv \bar{m}^a \nabla_a$ are derivative operators and $\kappa, \rho, \sigma, \tau, \nu, \mu, \lambda, \pi, \varepsilon, \beta, \gamma, \alpha$ are the spin coefficients. With the Kerr metric in BL coordinates (9), it can be written as

$$\begin{aligned} & \left[\frac{(r^2 + a^2)^2}{\Delta_r} - a^2 \sin^2 \theta \right] \frac{\partial^2 \psi}{\partial t^2} + \frac{4Mar}{\Delta_r} \frac{\partial^2 \psi}{\partial t \partial \varphi} + \left[\frac{a^2}{\Delta_r} - \frac{1}{\sin^2 \theta} \right] \frac{\partial^2 \psi}{\partial \varphi^2} - \frac{\partial}{\partial r} \left(\Delta_r \frac{\partial \psi}{\partial r} \right) - \frac{1}{\sin \theta} \frac{\partial}{\partial \theta} \left(\sin \theta \frac{\partial \psi}{\partial \theta} \right) \\ & + \frac{2M\rho^2}{\bar{\rho}} \psi = \frac{1}{\bar{\rho}} \left\{ [\Delta + (\bar{\mu} - \mu - \gamma - \bar{\gamma})] \frac{J_l}{\rho^2} + [\bar{\delta} - (\bar{\tau} + 2\alpha)] \frac{J_m}{\rho^2} \right\}, \end{aligned} \quad (25)$$

where $\psi = \varphi_1/\rho$, $J_l = J_\mu l^\mu$ and $J_m = J_\mu m^\mu$. The other two decoupled equations for φ_0 and φ_2 with sources can be found in [31].

In fact, in the scenario we are considering, the axion cloud is the source for the induced EM field that

$$\nabla_\nu F_{(1)}^{\mu\nu} = -2\nabla_\nu \phi_{(0)} {}^* F_{(0)}^{\mu\nu} \equiv J_{(1)}^\mu. \quad (26)$$

We can take a good approximation to the bound states of axion cloud around a rotating black hole [12]

$$\phi_{(0)} = \alpha_1^2 \phi_0 \frac{r}{M} e^{-\frac{r}{2M} \alpha_1^2} \cos(\varphi - \omega_R t) \sin \theta, \quad (27)$$

which is valid for $\alpha \lesssim 0.2$ even at large black hole spin, and $\omega_R \simeq \mu_1$ is the oscillating frequency.

It can be separated into two parts

$$\phi_1 = e^{-i\omega t + i\varphi} R(r) S(\theta), \quad \phi_2 = e^{i\omega t - i\varphi} R(r) S(\theta), \quad (28)$$

with $R(r) = \alpha_1^2 \phi_0 \frac{r}{2M} e^{-\frac{r}{2M} \alpha_1^2}$ and $S(\theta) = \sin \theta$.

Using ϕ_1 as the source and the NP scalars as partly separable variables

$$\varphi_{01} = e^{-i\omega_1 t + im_1 \varphi} f_{01}(r, \theta), \quad \varphi_{11} = e^{-i\omega_1 t + im_1 \varphi} f_{11}(r, \theta), \quad \varphi_{21} = e^{-i\omega_1 t + im_1 \varphi} f_{21}(r, \theta), \quad (29)$$

we can obtain the three decoupled differential equations respectively for $f_{01}(r, \theta)$, $f_{11}(r, \theta)$ and $f_{21}(r, \theta)$ after dropping off the time t and azimuthal angle φ dependence by $\omega_1 = \omega$ and $m_1 = m = 1$. We can also do that for ϕ_2 .

We replace $\omega = \mu_1 = \alpha_1/M$, $a_0 \equiv a/M$, $r_0 \equiv r/M$, and define new dimensionless quantities $f_{01M} \equiv M f_{01}(r, \theta)$, $f_{11M} \equiv M f_{11}(r, \theta)$, $f_{21M} \equiv M f_{21}(r, \theta)$. After absorbing some coefficients from the source part into the coupling constant k_a , we now use a new dimensionless coupling constant $\varepsilon \equiv \alpha_1^2 B_0 M \phi_0 k_a$ as the small quantity for expansion, then the new field equations are dimensionless

$$\text{eq}_{f_{01M}} : \left\{ \frac{\partial^2 f_{01M}(r_0, \theta)}{\partial r_0^2}, \frac{\partial f_{01M}(r_0, \theta)}{\partial r_0}, \frac{\partial^2 f_{01M}(r_0, \theta)}{\partial \theta^2}, \frac{\partial f_{01M}(r_0, \theta)}{\partial \theta}, f_{01M}(r_0, \theta), a_0, \alpha_1 \right\}, \quad (30)$$

$$\text{eq}_{f_{11M}} : \left\{ \frac{\partial^2 f_{11M}(r_0, \theta)}{\partial r_0^2}, \frac{\partial f_{11M}(r_0, \theta)}{\partial r_0}, \frac{\partial^2 f_{11M}(r_0, \theta)}{\partial \theta^2}, \frac{\partial f_{11M}(r_0, \theta)}{\partial \theta}, f_{11M}(r_0, \theta), a_0, \alpha_1 \right\}, \quad (31)$$

$$\text{eq}_{f_{21M}} : \left\{ \frac{\partial^2 f_{21M}(r_0, \theta)}{\partial r_0^2}, \frac{\partial f_{21M}(r_0, \theta)}{\partial r_0}, \frac{\partial^2 f_{21M}(r_0, \theta)}{\partial \theta^2}, \frac{\partial f_{21M}(r_0, \theta)}{\partial \theta}, f_{21M}(r_0, \theta), a_0, \alpha_1 \right\}, \quad (32)$$

and there are only two dimensionless parameters a_0 and α_1 .

Different from the quasi-normal modes and bound states, here the frequency of the induced EM field is already fixed by the frequency of the source (axion cloud), it is not an eigenvalue problem and no boundary condition should be imposed. Actually we can obtain the asymptotic behaviors of the functions at the boundaries by expanding the equations (we choose decaying solutions at spatial infinity), and then solve the equations numerically.

With expansions and the regular condition at poles $\theta = 0, \pi$, the asymptotic behaviors at the boundaries $r_0 = r_{h0} \equiv 1 + \sqrt{1 - a_0^2}$, $r_0 \rightarrow \infty$, $\theta = 0, \pi$ are as follows

$$f_{01M}(r_{h0}, \theta) = \frac{2\sqrt{2}a_0r_{h0}^3e^{-\alpha_1^2r_{h0}/2}\sin\theta\sin 2\theta}{\left(2\alpha_1r_{h0} - a_0 - 2i\sqrt{1 - a_0^2}\right)(r_{h0}^2 + a_0^2\cos^2\theta)^2}, \quad (33)$$

$$f_{11M}(r_{h0}, \theta) = \frac{2i\sqrt{1 - a_0^2}r_{h0}^3e^{-\alpha_1^2r_{h0}/2}\sin 2\theta}{(a_0 - 2\alpha_1r_{h0})(r_{h0}^2 + a_0^2\cos^2\theta)^2}, \quad (34)$$

$$f_{21M}(r_{h0}, \theta) = 0, \quad (35)$$

$$f_{01M}(r_0 \rightarrow \infty, \theta) = -\frac{3i\sin^2\theta e^{-\alpha_1^2r_0/2}}{\sqrt{2}\alpha_1} + \mathcal{O}\left(r_0^{-1}e^{-\alpha_1^2r_0/2}\right), \quad (36)$$

$$f_{11M}(r_0 \rightarrow \infty, \theta) = -\frac{(\alpha_1 + 3i)\sin 2\theta e^{-\alpha_1^2r_0/2}}{4\alpha_1} + \mathcal{O}\left(r_0^{-1}e^{-\alpha_1^2r_0/2}\right), \quad (37)$$

$$f_{21M}(r_0 \rightarrow \infty, \theta) = -\frac{3i\sin^2\theta e^{-\alpha_1^2r_0/2}}{2\sqrt{2}\alpha_1} + \mathcal{O}\left(r_0^{-1}e^{-\alpha_1^2r_0/2}\right), \quad (38)$$

$$f_{01M}(r_0, 0) = 0, \quad f_{11M}(r_0, 0) = 0, \quad f_{21M}(r_0, 0) = 0, \quad (39)$$

$$f_{01M}(r_0, \pi) = 0, \quad f_{11M}(r_0, \pi) = 0, \quad f_{21M}(r_0, \pi) = 0, \quad (40)$$

where the outgoing part $f_{21M}(r_0, \theta)$ just vanishes at the horizon in accord with the fact that there is no outgoing radiation at the event horizon. It should also result from the fact that φ_2 is with negative spin weight which can not retrograde against the rotation at event horizon.

In addition, it is clear that the asymptotic behaviors for f_{01M} and f_{11M} at event horizon r_{h0} are only valid when $\alpha_1 \neq \frac{a_0}{2r_{h0}}$, which is exactly the critical condition for whether superradiance occurs. In this critical case with $\alpha_1 = \frac{a_0}{2r_{h0}}$, the imaginary part ω_I disappears in the original field equation for the axion field, so that the whole frequency is not complex and the original boundary condition at event horizon is not valid, in which case another regular condition at origin should be applied. Here we do not go further on this case.

Similarly, for the NP scalars induced from ϕ_2

$$\varphi_{02} = e^{i\omega_1 t - im_1 \varphi} f_{02}(r, \theta), \quad \varphi_{12} = e^{i\omega_1 t - im_1 \varphi} f_{12}(r, \theta), \quad \varphi_{22} = e^{i\omega_1 t - im_1 \varphi} f_{22}(r, \theta), \quad (41)$$

we can get the corresponding equations and boundary conditions for $f_{02M}(r_0, \theta)$, $f_{12M}(r_0, \theta)$, $f_{22M}(r_0, \theta)$.

From the analysis of the equations, we found that the induced NP scalars from the two parts ϕ_1 and ϕ_2 of the axion cloud have following relations (here we remove the coefficient M)

$$\text{Re}[f_{01}(r, \theta)] = \text{Re}[f_{02}(r, \pi - \theta)], \quad \text{Im}[f_{01}(r, \theta)] = -\text{Im}[f_{02}(r, \pi - \theta)], \quad (42)$$

$$\text{Re}[f_{11}(r, \theta)] = -\text{Re}[f_{12}(r, \pi - \theta)], \quad \text{Im}[f_{11}(r, \theta)] = \text{Im}[f_{12}(r, \pi - \theta)], \quad (43)$$

$$\text{Re}[f_{21}(r, \theta)] = \text{Re}[f_{22}(r, \pi - \theta)], \quad \text{Im}[f_{21}(r, \theta)] = -\text{Im}[f_{22}(r, \pi - \theta)], \quad (44)$$

which means that with the above transformations, we can start from one set of the equations to the other set. These symmetries from analysis are consistent with the numerical results, thus here we only exhibit the distribution for those from ϕ_1 in FIG. 1.

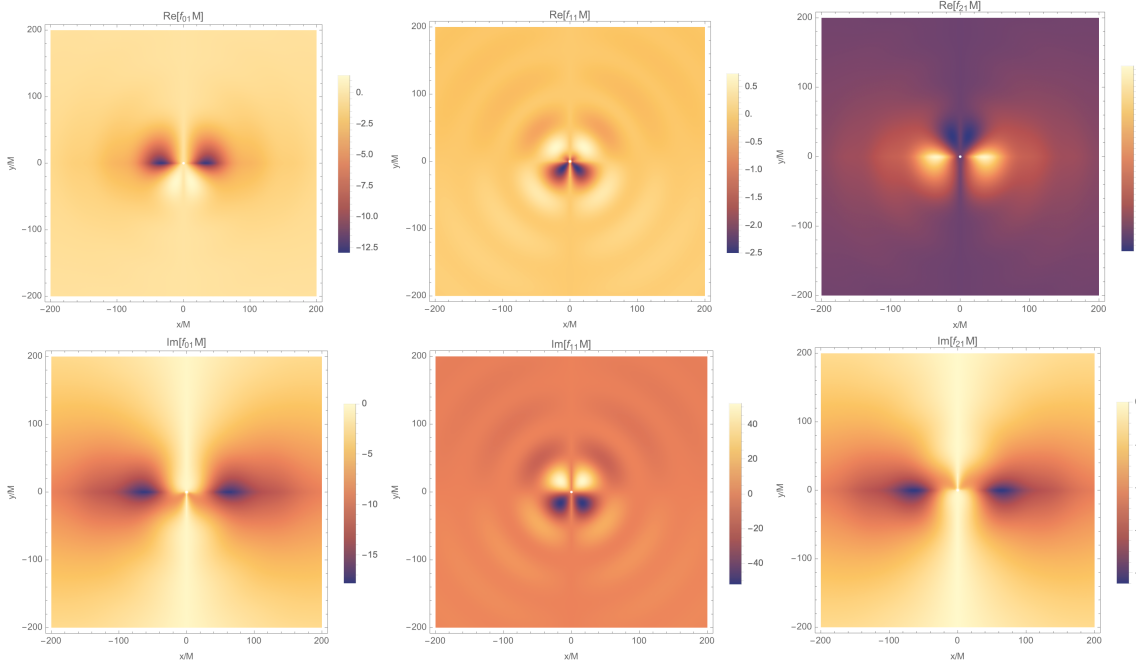


FIG. 1. The real and imaginal parts of $f_{01M}(r_0, \theta)$, $f_{11M}(r_0, \theta)$, $f_{21M}(r_0, \theta)$ induced from ϕ_1 are plotted with $a_0 = 0.5$ and $\alpha_1 = 0.1$ in the scale of $200M$, where the superradiant condition is satisfied $\alpha_1 < \frac{a_0}{2r_{h0}}$.

From FIG. 1 we can see that, the ingoing radiation f_{01M} is slightly larger than the outgoing radiation f_{21M} , and the residential part f_{11M} presents a ripple-like pattern. Usually the residential φ_1 part is neglected, since its equation is not separable even without any source and it is not related to ingoing or outgoing part. But here, it is shown that the imaginary part of f_{11M} gets much larger amplitude than the other parts, indicating that the residential part is the primary constituent of the EM photon cloud we are studying. In fact, both φ_0 and φ_2 contain ingoing and outgoing parts, people assign ingoing/outgoing radiation to φ_0/φ_2 due to which one is dominant at spatial infinity.

Subsequently, we can construct the EM tensor induced from ϕ_1 using (19)

$$F_{\mu\nu}^1 = 4 \cos(m\varphi - \omega t) \text{Re} [P_{\mu\nu}^1(r, \theta)] - 4 \sin(m\varphi - \omega t) \text{Im} [P_{\mu\nu}^1(r, \theta)] , \quad (45)$$

$$P_{\mu\nu}^1(r, \theta) \equiv f_{01}(r, \theta) \bar{m}_{[\mu} n_{\nu]} + f_{11}(r, \theta) n_{[\mu} l_{\nu]} + f_{11}(r, \theta) m_{[\mu} \bar{m}_{\nu]} + f_{21}(r, \theta) l_{[\mu} m_{\nu]} . \quad (46)$$

Similarly, for the EM tensor induced from ϕ_2 we have

$$F_{\mu\nu}^2 = 4 \cos(m\varphi - \omega t) \text{Re} [P_{\mu\nu}^2(r, \theta)] + 4 \sin(m\varphi - \omega t) \text{Im} [P_{\mu\nu}^2(r, \theta)] , \quad (47)$$

$$P_{\mu\nu}^2(r, \theta) \equiv f_{02}(r, \theta) \bar{m}_{[\mu} n_{\nu]} + f_{12}(r, \theta) n_{[\mu} l_{\nu]} + f_{12}(r, \theta) m_{[\mu} \bar{m}_{\nu]} + f_{22}(r, \theta) l_{[\mu} m_{\nu]} , \quad (48)$$

then the whole EM field induced from the axion cloud $\phi_{(0)} = \phi_1 + \phi_2$ evolves as

$$F_{\mu\nu}^{(1)} = F_{\mu\nu}^1 + F_{\mu\nu}^2 = \cos(m\varphi - \omega t) F_{\mu\nu}^{\cos}(r, \theta) + \sin(m\varphi - \omega t) F_{\mu\nu}^{\sin}(r, \theta) , \quad (49)$$

$$F_{\mu\nu}^{\cos}(r, \theta) = 4 \text{Re} [(f_{01} + f_{02}) \bar{m}_{[\mu} n_{\nu]} + (f_{11} + f_{12}) (n_{[\mu} l_{\nu]} + m_{[\mu} \bar{m}_{\nu]}) + (f_{21} + f_{22}) l_{[\mu} m_{\nu]}] , \quad (50)$$

$$F_{\mu\nu}^{\sin}(r, \theta) = 4 \text{Im} [(f_{02} - f_{01}) \bar{m}_{[\mu} n_{\nu]} + (f_{12} - f_{11}) (n_{[\mu} l_{\nu]} + m_{[\mu} \bar{m}_{\nu]}) + (f_{22} - f_{21}) l_{[\mu} m_{\nu]}] . \quad (51)$$

So far we have considered an EM photon cloud sourced by an axion cloud surrounding a Kerr black hole which is described by (49). This is one of the main results of our work. Moreover, it means that for an arbitrary current $J^a = e^{\pm i\omega t \mp i m \varphi} S(r, \theta)$ as the source we will always get a photon cloud evolving as

$$F_{\mu\nu} = 4 \cos(m\varphi - \omega t) \text{Re} [P_{\mu\nu}(r, \theta)] \pm 4 \sin(m\varphi - \omega t) \text{Im} [P_{\mu\nu}(r, \theta)] .$$

In fact, even for photons without any couplings, they can have an effective mass given by plasma and make superradiance to happen [32, 33].

IV. THE INDUCED ELECTRIC AND MAGNETIC FIELDS

In this Section we will study the induced electric field and magnetic field respectively. Considering the $(3+1)$ -decomposition of the spacetime [34]

$$ds^2 = -\alpha^2 dt^2 + \gamma_{ij} (dx^i + \beta^i dt) (dx^j + \beta^j dt) , \quad (52)$$

where β^i is shift vector, γ_{ij} is the spatial metric and the lapse function $\alpha = \sqrt{\frac{\Delta_r \Sigma}{\Delta_r \Sigma + 2Mr(a^2 + r^2)}}$ in Kerr metric (9). We can define the electric field and magnetic field [35]

$$E^a := n_b F^{ab} , \quad B^a := n_b {}^* F^{ab} , \quad (53)$$

with respect to an Eulerian observer $n^a = (1/\alpha, -\beta^i/\alpha)$ whose worldline is orthogonal to the spacelike hypersurface.

Therefore we have

$$E_{(1)}^i = \cos(m\varphi - \omega t) E_{\cos}^i(r, \theta) + \sin(m\varphi - \omega t) E_{\sin}^i(r, \theta) , \quad (54)$$

$$B_{(1)}^i = \cos(m\varphi - \omega t) B_{\cos}^i(r, \theta) + \sin(m\varphi - \omega t) B_{\sin}^i(r, \theta) , \quad (55)$$

where

$$E_{\cos}^i = -\alpha F_{\cos}^{i0} , \quad E_{\sin}^i = -\alpha F_{\sin}^{i0} , \quad (56)$$

$$B_{\cos}^i = -\frac{1}{2} \alpha \epsilon^{i0jk} F_{jk}^{\cos} , \quad B_{\sin}^i = -\frac{1}{2} \alpha \epsilon^{i0jk} F_{jk}^{\sin} . \quad (57)$$

In FIG. 2-4, we plot the components of induced electric and magnetic fields in cosine and sine sections respectively, in contrast with the background Wald case. In some panels with large scale like $100M$, we use the dotted circles to denote the radius $r_{\max}/M = 2/\alpha_1^2$ of the maximum value of axion cloud, while in some panels with small scale like $5M$, we compare with the boundary of photon region (dotdashed curves) and event horizon (dashed circles). It is a good case to compare the distribution of the EMs (in field perspective) with the photon region (spherical photon orbits in particle perspective).

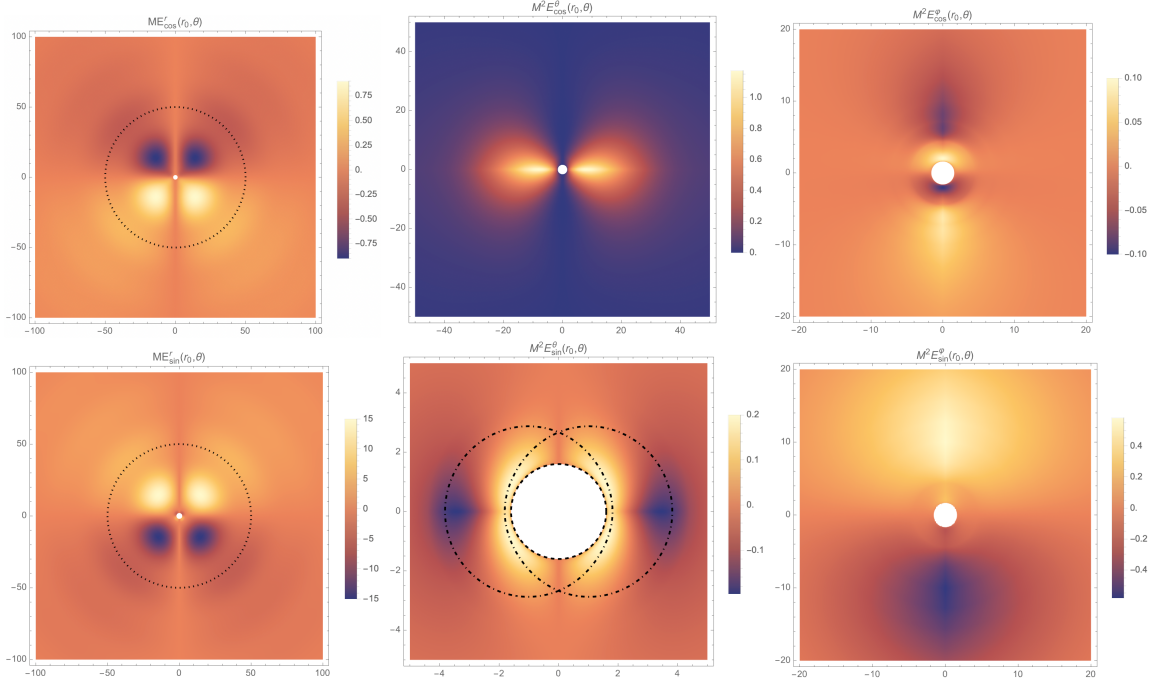


FIG. 2. The components of the induced electric fields are plotted as cosine part and sine part respectively. In all the figures we have set $a_0 = 0.8$ and $\alpha_1 = 0.2$.

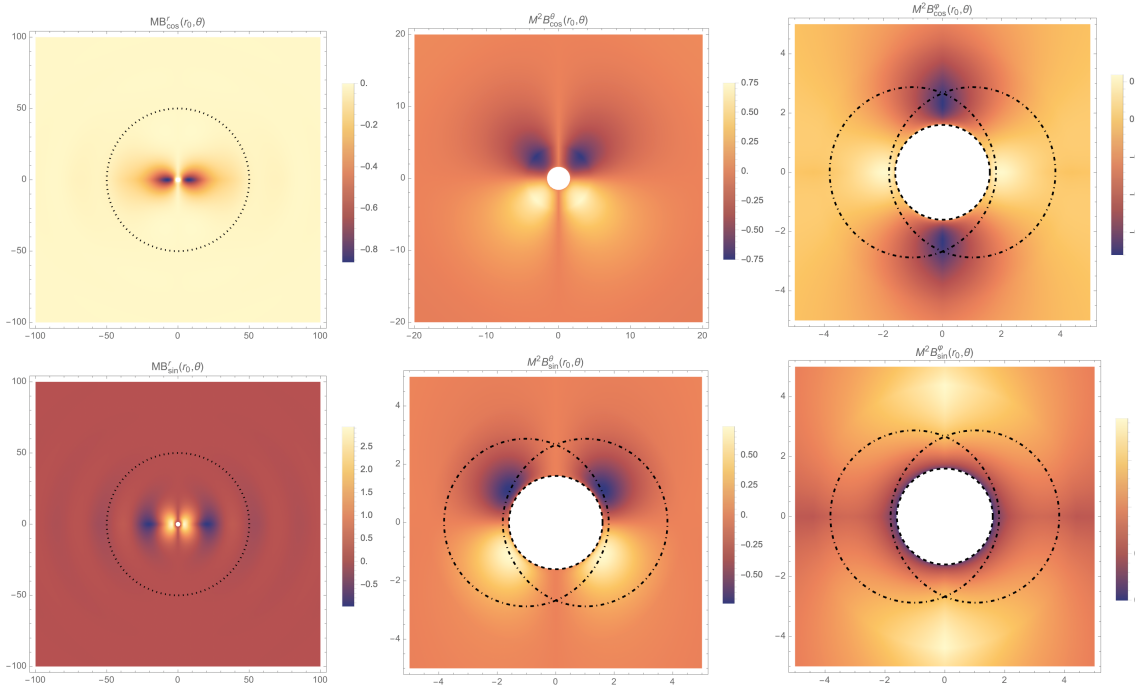


FIG. 3. The components of the induced magnetic fields are plotted as cosine part and sine part respectively. In all the figures we have set $a_0 = 0.8$ and $\alpha_1 = 0.2$.

From the figures we can see that, the radial components E_{\cos}^r and E_{\sin}^r of the induced electric field both exhibit quadrupole moments with a parity violation ($P = -1$). In contrast, the radial component of electric field of the background Wald case is in dipole moments with a parity symmetry ($P = +1$). While the θ components E_{\cos}^θ and E_{\sin}^θ of the induced electric field both exhibit a parity symmetry ($P = +1$). In contrast, the θ component of electric field of the background Wald case is in quadrupole moments with a parity violation ($P = -1$). For the φ components E_{\cos}^φ and E_{\sin}^φ of the induced electric field, they both show a parity violation symmetry ($P = -1$). Conversely, the symmetries for the components of magnetic fields are all opposite with those for electric fields. Besides, we can observe some evident coincides between the distribution of the induced electric and magnetic fields and the boundary of photon region.

Note that both electric and magnetic fields of the background Wald case do not contain φ components, and they only distribute outside the ergoregion, while the induced EM field can live within the ergoregion. This can be understood as “no static observer is allowed inside the ergoregion”.

As we know, superradiance only happens for massive fields, where the mass term makes them gathering around the black hole and sustainably dissipate near the event horizon. The dissipation is a crucial ingredient for superradiance, in fact even for a rotating compact object without a horizon, superradiance can occur via other dissipation mechanism, like friction [10].

While for the axion-photon coupling case, due to the antisymmetry of $\epsilon^{\mu\nu\rho\sigma}$ there is never an effective mass term for the photons, though sometimes people call it “tachyonic-like instability” [20]. Also it has been mentioned that the time-dependent axion is a crucial ingredient to trigger this instability when $k_a\phi_0$ is larger than a critical value.

In our first-order study with an EM background, even for small couplings, the exponential growing happens for the EM field coupled to the axion field, as we have discussed in Sec. II. From our perspective, the reason is that the stationary axion cloud ties the EM field onto the nearby of the black hole and serves as a source continuously, which makes the EM field dissipate sustainably from the axion cloud to the photon region and finally to the event horizon. As it is shown in the figures, the induced EM field does not concentrate around the maximum value of axion cloud but its main distribution is inside the dotted circles. In other words, the most dense places for the photon cloud do not relate to the largest oscillating position (same radius r_{\max}) of the axion cloud but inside it.

V. ANALYSIS OF SYMMETRIES AND PARITY VIOLATION

It is well known that the term $F_{\mu\nu}^* F^{\mu\nu}$ violates parity and couples to the pseudo-scalar axion field, making the whole term $\phi F_{\mu\nu}^* F^{\mu\nu}$ parity invariant and leading to CP violation.

Here in curved spacetime and classically, we obtain the same symmetry for the parity violation ($P = -1$). From (49), we have

$$\begin{aligned} F_{\mu\nu}^{(1)*} F_{(1)}^{\mu\nu} &= \cos^2(m\varphi - \omega t) F_{\mu\nu}^{\cos*} F_{\cos}^{\mu\nu} + \sin^2(m\varphi - \omega t) F_{\mu\nu}^{\sin*} F_{\sin}^{\mu\nu} + 2 \cos(m\varphi - \omega t) \sin(m\varphi - \omega t) F_{\mu\nu}^{\cos*} F_{\sin}^{\mu\nu} \\ &= \cos(2m\varphi - 2\omega t) \left(\frac{1}{2} F_{\mu\nu}^{\cos*} F_{\cos}^{\mu\nu} - \frac{1}{2} F_{\mu\nu}^{\sin*} F_{\sin}^{\mu\nu} \right) + \sin(2m\varphi - 2\omega t) F_{\mu\nu}^{\cos*} F_{\sin}^{\mu\nu} + \frac{1}{2} F_{\mu\nu}^{\cos*} F_{\cos}^{\mu\nu} + \frac{1}{2} F_{\mu\nu}^{\sin*} F_{\sin}^{\mu\nu}, \end{aligned} \quad (58)$$

where $m = 1$ and

$$\begin{aligned} F_{\mu\nu}^{\cos*} F_{\cos}^{\mu\nu} &= 8[(\text{Im}[f_{01}] + \text{Im}[f_{02}])(\text{Re}[f_{21}] + \text{Re}[f_{22}]) + (\text{Re}[f_{01}] + \text{Re}[f_{02}])(\text{Im}[f_{21}] + \text{Im}[f_{22}]) \\ &\quad - 2(\text{Im}[f_{11}] + \text{Im}[f_{12}])(\text{Re}[f_{11}] + \text{Re}[f_{12}])], \end{aligned} \quad (59)$$

$$\begin{aligned} F_{\mu\nu}^{\sin*} F_{\sin}^{\mu\nu} &= -8(\text{Im}[f_{01}] - \text{Im}[f_{02}])(\text{Re}[f_{21}] - \text{Re}[f_{22}]) - 8(\text{Re}[f_{01}] - \text{Re}[f_{02}])(\text{Im}[f_{21}] - \text{Im}[f_{22}]) \\ &\quad + 16(\text{Im}[f_{11}] - \text{Im}[f_{12}])(\text{Re}[f_{11}] - \text{Re}[f_{12}]), \end{aligned} \quad (60)$$

$$\begin{aligned} F_{\mu\nu}^{\cos*} F_{\sin}^{\mu\nu} &= 8[-\text{Im}[f_{01}]\text{Im}[f_{21}] + \text{Re}[f_{01}]\text{Re}[f_{21}] + \text{Im}[f_{02}]\text{Im}[f_{22}] - \text{Re}[f_{02}]\text{Re}[f_{22}] \\ &\quad + \text{Im}[f_{11}]^2 - \text{Re}[f_{11}]^2 - \text{Im}[f_{12}]^2 + \text{Re}[f_{12}]^2], \end{aligned} \quad (61)$$

all exhibit a sign change for $\theta \rightarrow \pi - \theta$, in agreement with the results in FIG. 5. Combined with no sign change for $\varphi \rightarrow \varphi + \pi$, we know that there is a parity violation $P = -1$ for $F_{\mu\nu}^{(1)*} F_{(1)}^{\mu\nu}$.

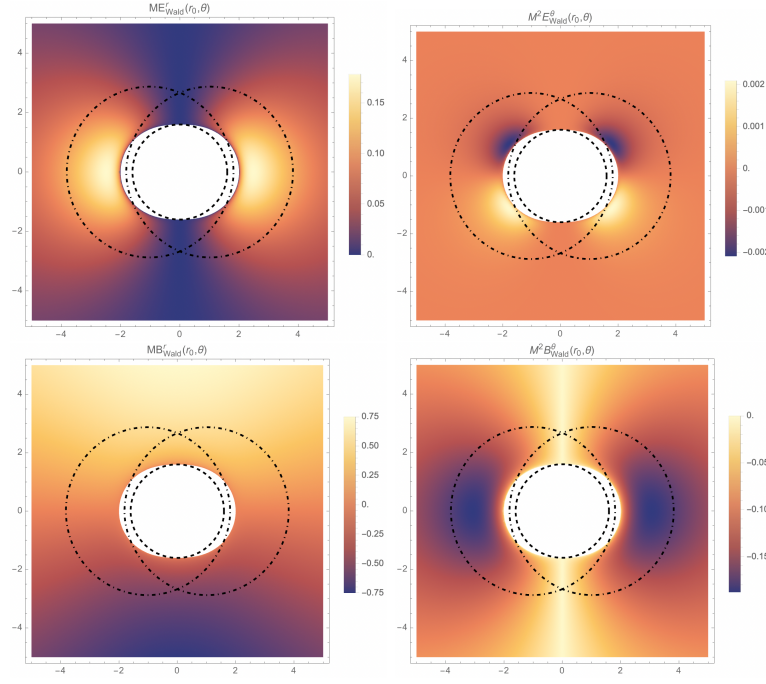


FIG. 4. The components of the electric and magnetic fields are plotted for the background Wald case, where we have set $a_0 = 0.8$ and $\alpha_1 = 0.2$.

In addition, it shows that except for the evolving parts with a double frequency 2ω , there are also residential parts that are time-independent.

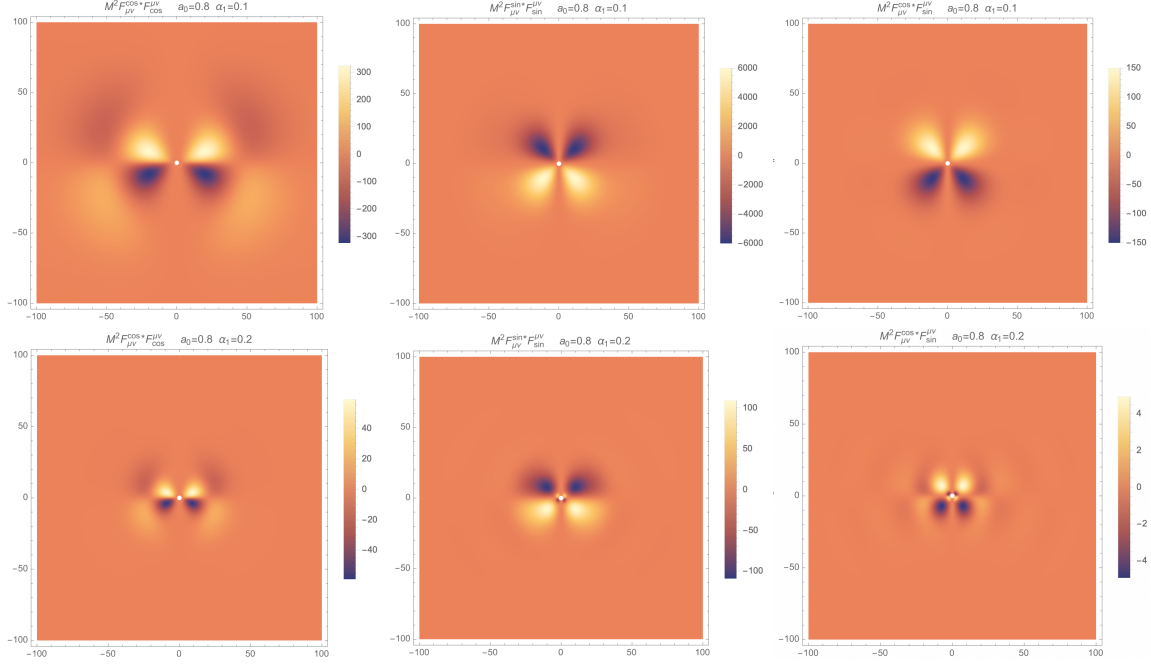


FIG. 5. The components $M^2 F_{\mu\nu}^{\cos*} F_{\cos}^{\mu\nu}$, $M^2 F_{\mu\nu}^{\sin*} F_{\sin}^{\mu\nu}$, $M^2 F_{\mu\nu}^{\cos*} F_{\sin}^{\mu\nu}$ of the parity violation term $M^2 F_{\mu\nu}^{(1)*} F_{(1)}^{\mu\nu}$ are plotted with $a_0 = 0.8$ and $\alpha_1 = 0.1, 0.2$.

Similarly, the contraction of the EM field strength tensor $F_{\mu\nu}^{(1)} F_{(1)}^{\mu\nu}$ evolves as

$$\begin{aligned} F_{\mu\nu}^{(1)} F_{(1)}^{\mu\nu} &= \cos^2(m\varphi - \omega t) F_{\mu\nu}^{\cos} F_{\cos}^{\mu\nu} + \sin^2(m\varphi - \omega t) F_{\mu\nu}^{\sin} F_{\sin}^{\mu\nu} + 2 \cos(m\varphi - \omega t) \sin(m\varphi - \omega t) F_{\mu\nu}^{\cos} F_{\sin}^{\mu\nu} \quad (62) \\ &= \cos(2m\varphi - 2\omega t) \left(\frac{1}{2} F_{\mu\nu}^{\cos} F_{\cos}^{\mu\nu} - \frac{1}{2} F_{\mu\nu}^{\sin} F_{\sin}^{\mu\nu} \right) + \sin(2m\varphi - 2\omega t) F_{\mu\nu}^{\cos} F_{\sin}^{\mu\nu} + \frac{1}{2} F_{\mu\nu}^{\cos} F_{\cos}^{\mu\nu} + \frac{1}{2} F_{\mu\nu}^{\sin} F_{\sin}^{\mu\nu}, \end{aligned}$$

where $m = 1$ and

$$\begin{aligned} F_{\mu\nu}^{\cos} F_{\cos}^{\mu\nu} &= 8 [-(\text{Im}[f_{01}] + \text{Im}[f_{02}])(\text{Im}[f_{21}] + \text{Im}[f_{22}]) + (\text{Re}[f_{01}] + \text{Re}[f_{02}]) (\text{Re}[f_{21}] + \text{Re}[f_{22}]) \\ &\quad + (\text{Im}[f_{11}] + \text{Im}[f_{12}])^2 - (\text{Re}[f_{11}] + \text{Re}[f_{12}])^2], \quad (63) \end{aligned}$$

$$\begin{aligned} F_{\mu\nu}^{\sin} F_{\sin}^{\mu\nu} &= 8 [(\text{Im}[f_{01}] - \text{Im}[f_{02}])(\text{Im}[f_{21}] - \text{Im}[f_{22}]) - (\text{Re}[f_{01}] - \text{Re}[f_{02}]) (\text{Re}[f_{21}] - \text{Re}[f_{22}]) \\ &\quad - (\text{Im}[f_{11}] - \text{Im}[f_{12}])^2 + (\text{Re}[f_{11}] - \text{Re}[f_{12}])^2], \quad (64) \end{aligned}$$

$$\begin{aligned} F_{\mu\nu}^{\cos} F_{\sin}^{\mu\nu} &= 8 [-\text{Im}[f_{01}] \text{Re}[f_{21}] - \text{Re}[f_{01}] \text{Im}[f_{21}] + \text{Im}[f_{02}] \text{Re}[f_{22}] + \text{Re}[f_{02}] \text{Im}[f_{22}] \\ &\quad + 2 \text{Im}[f_{11}] \text{Re}[f_{11}] - 2 \text{Im}[f_{12}] \text{Re}[f_{12}]], \quad (65) \end{aligned}$$

all keep a parity symmetry $P = +1$ under $\theta \rightarrow \pi - \theta$, in agreement with the results in FIG. 6. Also there is no sign change under $\varphi \rightarrow \varphi + \pi$, hence the whole $F_{\mu\nu}^{(1)} F_{(1)}^{\mu\nu}$ keeps parity symmetry $P = +1$.

We know that the null conditions for EM fields are $F_{\mu\nu} F^{\mu\nu} = 0$ and $F_{\mu\nu}^* F^{\mu\nu} = 0$, which is equivalent to $\varphi_0 \varphi_2 - \varphi_1^2 = 0$. Here with the axion-photon coupling, it shows obviously that the null conditions are not satisfied anymore.

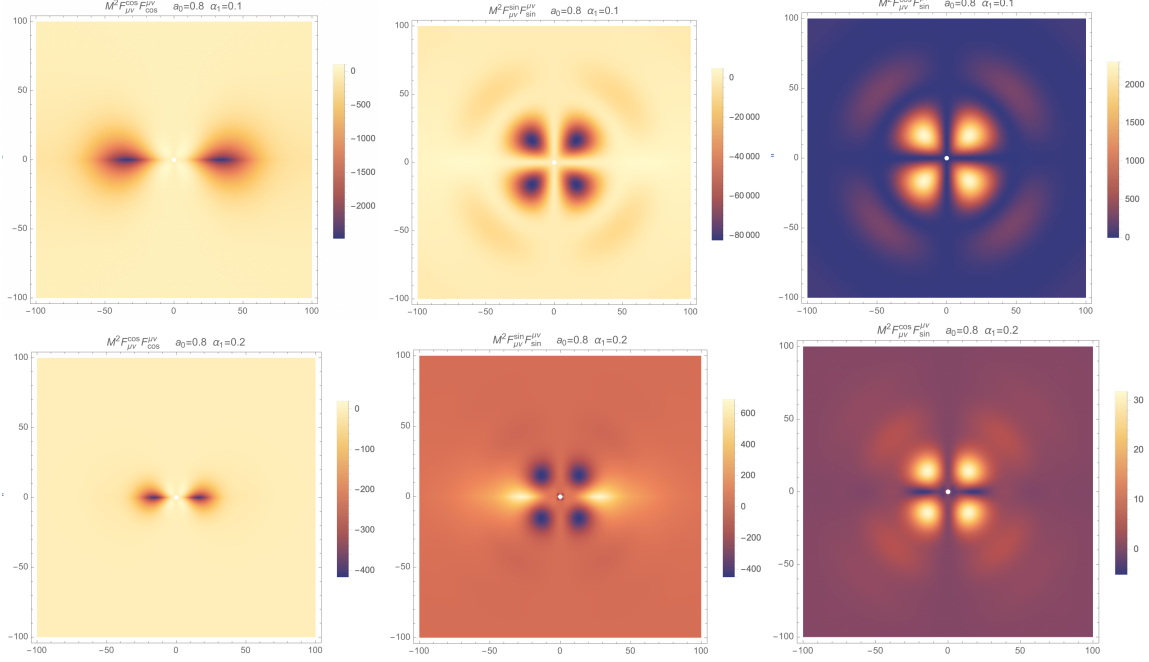


FIG. 6. The components $M^2 F_{\mu\nu}^{\cos} F_{\cos}^{\mu\nu}$, $M^2 F_{\mu\nu}^{\sin} F_{\sin}^{\mu\nu}$, $M^2 F_{\mu\nu}^{\cos} F_{\sin}^{\mu\nu}$ of the contraction of the EM field strength tensor $M^2 F_{\mu\nu}^{(1)} F_{(1)}^{\mu\nu}$ are plotted with $a_0 = 0.8$ and $\alpha_1 = 0.1, 0.2$.

Moreover, we study the effects of the two parameters a_0 , α_1 and find that the spin parameter a_0 only has slight impacts on both the amplitude and the structure of the distribution for each components of $M^2 F_{\mu\nu}^{(1)} * F_{(1)}^{\mu\nu}$ and $M^2 F_{\mu\nu}^{(1)} F_{(1)}^{\mu\nu}$, while these quantities are sensitive to the fine structure constant α_1 . Therefore, in FIG. 5-6 we plot the figures for the components of $M^2 F_{\mu\nu}^{(1)} * F_{(1)}^{\mu\nu}$ and $M^2 F_{\mu\nu}^{(1)} F_{(1)}^{\mu\nu}$ with fixed $a_0 = 0.8$ and different values of α_1 . From the figures we can see that, for all the components, the increase of α_1 leads to a significant decrease in amplitude and a slight concentration on the distribution, which indicates that for fixed black hole mass M the smaller axion mass μ_1 (larger reduced Compton wavelength) makes the interaction with photons more efficient and stronger. Also, the slight concentration on the distribution should result from the concentration of the axion cloud with larger α_1 , where larger axion mass μ_1 (smaller reduced Compton wavelength) makes the axion cloud concentrate. In general, the induced EM scalars $M^2 F_{\mu\nu}^{(1)} * F_{(1)}^{\mu\nu}$ and $M^2 F_{\mu\nu}^{(1)} F_{(1)}^{\mu\nu}$ concentrate in the sine parts $M^2 F_{\mu\nu}^{\sin} * F_{\sin}^{\mu\nu}$ and $M^2 F_{\mu\nu}^{\sin} F_{\sin}^{\mu\nu}$.

For the electric and magnetic fields respectively, applying the relations (42)-(44), we can obtain some symmetries for the components in cosine and sine parts

$$E_{\cos/\sin}^r(r, \pi - \theta) = -E_{\cos}^r(r, \theta), \quad B_{\cos/\sin}^r(r, \pi - \theta) = B_{\cos/\sin}^r(r, \theta), \quad (66)$$

$$E_{\cos/\sin}^\theta(r, \pi - \theta) = E_{\cos/\sin}^\theta(r, \theta), \quad B_{\cos/\sin}^\theta(r, \pi - \theta) = -B_{\cos/\sin}^\theta(r, \theta), \quad (67)$$

$$E_{\cos/\sin}^\varphi(r, \pi - \theta) = -E_{\cos/\sin}^\varphi(r, \theta), \quad B_{\cos/\sin}^\varphi(r, \pi - \theta) = B_{\cos/\sin}^\varphi(r, \theta), \quad (68)$$

which can be clearly seen in FIG. 2-3. We further have

$$E_{(1)}^r(t, r, \pi - \theta, \varphi + \pi) = E_{(1)}^r(t, r, \theta, \varphi), \quad B_{(1)}^r(t, r, \pi - \theta, \varphi + \pi) = -B_{(1)}^r(t, r, \theta, \varphi), \quad (69)$$

$$E_{(1)}^\theta(t, r, \pi - \theta, \varphi + \pi) = -E_{(1)}^\theta(t, r, \theta, \varphi), \quad B_{(1)}^\theta(t, r, \pi - \theta, \varphi + \pi) = B_{(1)}^\theta(t, r, \theta, \varphi), \quad (70)$$

$$E_{(1)}^\varphi(t, r, \pi - \theta, \varphi + \pi) = E_{(1)}^\varphi(t, r, \theta, \varphi), \quad B_{(1)}^\varphi(t, r, \pi - \theta, \varphi + \pi) = -B_{(1)}^\varphi(t, r, \theta, \varphi), \quad (71)$$

and the background EM field transforms as

$$E_{(0)}^r(t, r, \pi - \theta, \varphi + \pi) = E_{(0)}^r(t, r, \theta, \varphi) \ , \quad B_{(0)}^r(t, r, \pi - \theta, \varphi + \pi) = -B_{(0)}^r(t, r, \theta, \varphi) \ , \quad (72)$$

$$E_{(0)}^\theta(t, r, \pi - \theta, \varphi + \pi) = -E_{(0)}^\theta(t, r, \theta, \varphi) \ , \quad B_{(0)}^\theta(t, r, \pi - \theta, \varphi + \pi) = B_{(0)}^\theta(t, r, \theta, \varphi) \ . \quad (73)$$

These transformations are equivalent to $\vec{E} \rightarrow -\vec{E}$ and $\vec{B} \rightarrow \vec{B}$ under $\vec{r} \rightarrow -\vec{r}$. Therefore the induced electric field still keep a parity symmetry with $P = -1$ as a vector, and the induced magnetic field keeps the parity symmetry with $P = +1$ as a pseudo-vector, same as the EM background.

In addition, we are interested in the strengths of the induced electric and magnetic fields that

$$\begin{aligned} E_{(1)}^i E_i^{(1)} &= \cos^2(m\varphi - \omega t) E_{\cos}^i E_i^{\cos} + \sin^2(m\varphi - \omega t) E_{\sin}^i E_i^{\sin} + 2 \cos(m\varphi - \omega t) \sin(m\varphi - \omega t) E_{\cos}^i E_i^{\sin} \quad (74) \\ &= \cos(2m\varphi - 2\omega t) \left(\frac{1}{2} E_{\cos}^i E_i^{\cos} - \frac{1}{2} E_{\sin}^i E_i^{\sin} \right) + \sin(2m\varphi - 2\omega t) E_{\cos}^i E_i^{\sin} + \frac{1}{2} E_{\cos}^i E_i^{\cos} + \frac{1}{2} E_{\sin}^i E_i^{\sin} \end{aligned}$$

which also works for $B_{(1)}^i B_i^{(1)}$.

We plot the strengths of electric and magnetic fields in different sections in FIG. 7, from which we can see that the strengths are mainly concentrated in E_{\cos}^2 , E_{\sin}^2 and B_{\sin}^2 , and for each panel there is a distinctive pattern of the distribution. It was mentioned in [31] that, when sources are present we can use the eigenfunctions of the angle-part equation to separate the master equation for φ_0 or φ_2 (their master equations without sources are separable) by expanding the source $T = \Sigma G(r)_s S_{lm}(\theta) e^{im\varphi} e^{-i\omega t}$. Remember that there are only two real degrees of freedom, i.e. once we get φ_0 or φ_2 then the other two complex quantities are decided. Therefore these featured patterns should come from the decomposition of the source, in our case it is the axion cloud but the expression of T is so complicate to expand one by one.

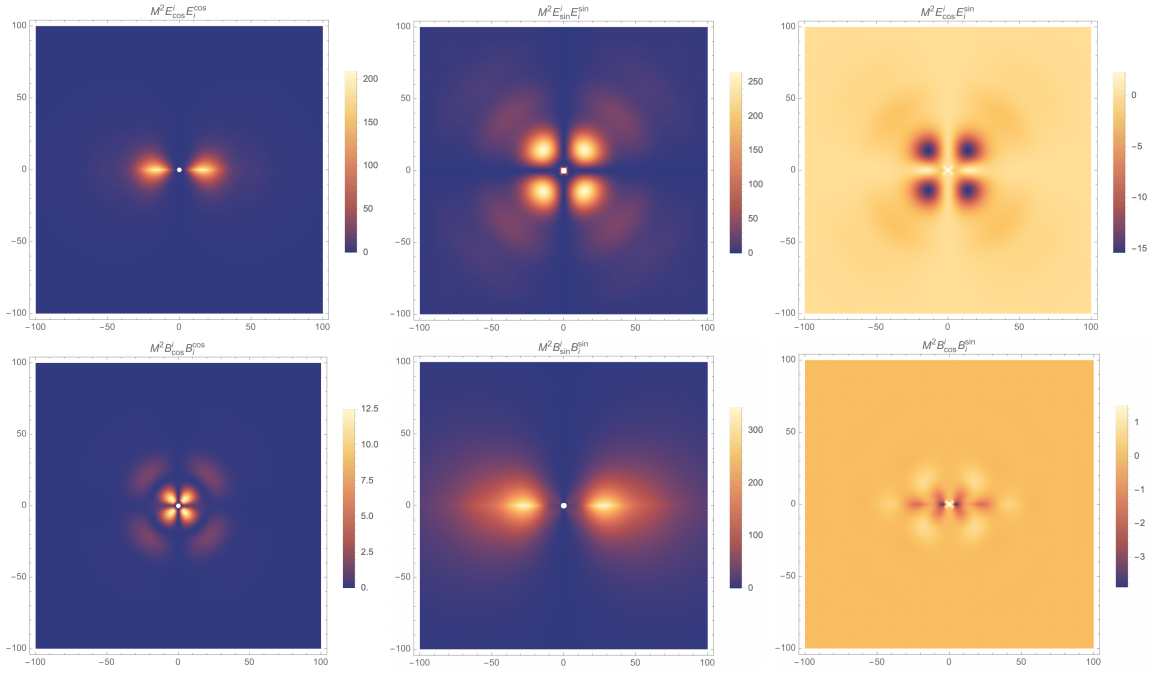


FIG. 7. The strengths of electric field and magnetic field $M^2 E_{\cos}^i E_i^{\cos}$, $M^2 E_{\sin}^i E_i^{\sin}$, $M^2 E_{\cos}^i E_i^{\sin}$, $M^2 B_{\cos}^i B_i^{\cos}$, $M^2 B_{\sin}^i B_i^{\sin}$, $M^2 B_{\cos}^i B_i^{\sin}$ are plotted with $a_0 = 0.8$ and $\alpha_1 = 0.2$.

VI. CONCLUSIONS

In this work we studied the EM photon cloud sourced by an axion cloud through the axion-photon coupling around a Kerr black hole in the presence of a background EM field. In the first-order study of the coupling constant, we obtained an oscillating EM photon cloud with the same frequency as the axion cloud, which indicates that it exists even for very small couplings with no threshold. More intriguingly, this induced EM photon cloud is growing exponentially in accordance with the axion cloud when the superradiant condition for the axion field is satisfied.

In addition, we studied the induced electric and magnetic fields respectively, and found that their components exhibit very different symmetries in contrast with the EM background, which may indicate the existence of both an axion cloud and the axion-photon coupling. Furthermore, we analyzed the symmetries of most quantities in curved spacetime and confirmed the parity violation $P = -1$ of the $F_{\mu\nu}^{(1)} * F_{(1)}^{\mu\nu}$ term. Besides, for near horizon region, we compared the distribution of the induced EM field with the boundary of photon region and found some overlap as expected.

ACKNOWLEDGMENTS

We thank Masahide Yamaguchi, Jin Sun, Yuhang Zhu and Cheng-Yong Zhang for beneficial discussions. This work is supported by IBS under the project code IBS-R018-D3.

-
- [1] R. D. Peccei and H. R. Quinn, “CP Conservation in the Presence of Instantons,” *Phys. Rev. Lett.* **38** (1977), 1440-1443.
 - [2] S. Weinberg, “A New Light Boson?,” *Phys. Rev. Lett.* **40** (1978), 223-226.
 - [3] F. Wilczek, “Problem of Strong P and T Invariance in the Presence of Instantons,” *Phys. Rev. Lett.* **40** (1978), 279-282.
 - [4] A. Arvanitaki, S. Dimopoulos, S. Dubovsky, N. Kaloper and J. March-Russell, “String Axiverse,” *Phys. Rev. D* **81**, 123530 (2010) [arXiv:0905.4720 [hep-th]].
 - [5] A. Arvanitaki and S. Dubovsky, “Exploring the String Axiverse with Precision Black Hole Physics,” *Phys. Rev. D* **83**, 044026 (2011) [arXiv:1004.3558 [hep-th]].
 - [6] D. J. E. Marsh, “Axion Cosmology,” *Phys. Rept.* **643** (2016), 1-79 [arXiv:1510.07633 [astro-ph.CO]].
 - [7] M. J. Duncan, N. Kaloper and K. A. Olive, “Axion hair and dynamical torsion from anomalies,” *Nucl. Phys. B* **387**, 215-235 (1992).
 - [8] P. Svrcek and E. Witten, “Axions In String Theory,” *JHEP* **06**, 051 (2006) [arXiv:hep-th/0605206 [hep-th]].
 - [9] T. F. M. Spieksma, E. Cannizzaro, T. Ikeda, V. Cardoso and Y. Chen, “Superradiance: Axionic couplings and plasma effects,” *Phys. Rev. D* **108** (2023) no.6, 063013 [arXiv:2306.16447 [gr-qc]].
 - [10] R. Brito, V. Cardoso and P. Pani, “Superradiance: New Frontiers in Black Hole Physics,” *Lect. Notes Phys.* **906**, pp.1-237 (2015) 2020, ISBN 978-3-319-18999-4, 978-3-319-19000-6, 978-3-030-46621-3, 978-3-030-46622-0 [arXiv:1501.06570 [gr-qc]].
 - [11] Y. Chen, X. Xue, R. Brito and V. Cardoso, “Photon Ring Astrometry for Superradiant Clouds,” *Phys. Rev. Lett.* **130** (2023) no.11, 111401 [arXiv:2211.03794 [gr-qc]].
 - [12] R. Brito, V. Cardoso and P. Pani, “Black holes as particle detectors: evolution of superradiant instabilities,” *Class. Quant. Grav.* **32** (2015) no.13, 134001 [arXiv:1411.0686 [gr-qc]].
 - [13] R. Penrose and R. M. Floyd, “Extraction of rotational energy from a black hole,” *Nature* **229**, 177 (1971).
 - [14] C. W. Misner, “Mixmaster universe,” *Phys. Rev. Lett.* **22**, 1071 (1969).
 - [15] S. A. Teukolsky, “Perturbations of a rotating black hole. 1. Fundamental equations for gravitational electromagnetic and neutrino field perturbations,” *Astrophys. J.* **185**, 635 (1973).
 - [16] R. M. Wald, “Black hole in a uniform magnetic field,” *Phys. Rev. D* **10** (1974), 1680-1685.
 - [17] J. D. Bekenstein, “Extraction of energy and charge from a black hole,” *Phys. Rev. D* **7**, 949 (1973).
 - [18] N. Siemonsen, C. Mondino, D. Egana-Ugrinovic, J. Huang, M. Baryakhtar and W. E. East, “Dark photon superradiance: Electrodynamics and multimessenger signals,” *Phys. Rev. D* **107** (2023) no.7, 075025 [arXiv:2212.09772 [astro-ph.HE]].

- [19] N. Siemonsen, T. May and W. E. East, “Modeling the black hole superradiance gravitational waveform,” *Phys. Rev. D* **107** (2023) no.10, 104003 [arXiv:2211.03845 [gr-qc]].
- [20] T. Ikeda, R. Brito and V. Cardoso, “Blasts of Light from Axions,” *Phys. Rev. Lett.* **122** (2019) no.8, 081101 [arXiv:1811.04950 [gr-qc]].
- [21] N. Chatzifotis, P. Dorlis, N. E. Mavromatos and E. Papantonopoulos, “Axion induced angular momentum reversal in Kerr-like black holes,” *Phys. Rev. D* **106**, no.8, 084002 (2022) [arXiv:2206.11734 [gr-qc]].
- [22] A. Arvanitaki, M. Baryakhtar and X. Huang, “Discovering the QCD Axion with Black Holes and Gravitational Waves,” *Phys. Rev. D* **91**, no.8, 084011 (2015) [arXiv:1411.2263 [hep-ph]].
- [23] T. W. Kephart and T. J. Weiler, “Luminous Axion Clusters,” *Phys. Rev. Lett.* **58** (1987), 171.
- [24] T. W. Kephart and T. J. Weiler, “Stimulated radiation from axion cluster evolution,” *Phys. Rev. D* **52** (1995), 3226-3238.
- [25] J. G. Rosa and T. W. Kephart, “Stimulated Axion Decay in Superradiant Clouds around Primordial Black Holes,” *Phys. Rev. Lett.* **120** (2018) no.23, 231102 [arXiv:1709.06581 [gr-qc]].
- [26] S. Sen, “Plasma effects on lasing of a uniform ultralight axion condensate,” *Phys. Rev. D* **98** (2018) no.10, 103012 [arXiv:1805.06471 [hep-ph]].
- [27] M. Boskovic, R. Brito, V. Cardoso, T. Ikeda and H. Witek, “Axionic instabilities and new black hole solutions,” *Phys. Rev. D* **99** (2019) no.3, 035006 [arXiv:1811.04945 [gr-qc]].
- [28] Y. Chen, Y. Liu, R. S. Lu, Y. Mizuno, J. Shu, X. Xue, Q. Yuan and Y. Zhao, “Stringent axion constraints with Event Horizon Telescope polarimetric measurements of M87*,” *Nature Astron.* **6** (2022) no.5, 592-598 [arXiv:2105.04572 [hep-ph]].
- [29] S. L. Detweiler, “Klein-Gordon equation and rotating black holes,” *Phys. Rev. D* **22** (1980), 2323-2326.
- [30] W. Kinnersley, “Type D Vacuum Metrics,” *J. Math. Phys.* **10** (1969), 1195-1203.
- [31] S. A. Teukolsky, “Rotating black holes - separable wave equations for gravitational and electromagnetic perturbations,” *Phys. Rev. Lett.* **29** (1972), 1114-1118.
- [32] P. Pani and A. Loeb, “Constraining Primordial Black-Hole Bombs through Spectral Distortions of the Cosmic Microwave Background,” *Phys. Rev. D* **88** (2013), 041301 [arXiv:1307.5176 [astro-ph.CO]].
- [33] H. Fukuda and K. Nakayama, “Aspects of Nonlinear Effect on Black Hole Superradiance,” *JHEP* **01** (2020), 128 [arXiv:1910.06308 [hep-ph]].
- [34] M. Alcubierre, “Introduction to 3 + 1 Numerical Relativity,” (Oxford University Press, New York, 2008).
- [35] M. Alcubierre, J. C. Degollado and M. Salgado, “The Einstein-Maxwell system in 3+1 form and initial data for multiple charged black holes,” *Phys. Rev. D* **80** (2009), 104022 [arXiv:0907.1151 [gr-qc]].